

ANTI-SWAY CONTROL OF TOWER CRANE BASED ON SLIDING MODE CONTROL

QingYun Zhang*, Qun Zhang, KeLong Xu
Jinan Wantian Machinery Equipment Co., Ltd, Jinan 250000, Shandong, China.
Corresponding Author: QingYun Zhang, Email: 417824279@qq.com

Abstract: In industrial applications, tower cranes, as crucial lifting equipment, play an essential role. However, due to their inherent underactuated nonlinear characteristics, cranes are often subject to inertial forces and external disturbances during actual operations, leading to load oscillations. Currently, the operation of tower cranes primarily relies on manual control by drivers, which is not only inefficient but also prone to causing residual oscillations in the loads, increasing the risk of safety incidents such as collisions and overturning. To address this issue, this paper proposes a sliding mode control-based method aimed at effectively suppressing the oscillations of the loads on tower cranes, ensuring the stability and reliability of their operation. Through simulation verification, this method provides a new technical solution for the efficient and safe operation of tower cranes.

Keywords: Tower crane; Sliding mode control

1 INTRODUCTION

In engineering practice, cranes typically use hooks as the core lifting device [1]. Since the hook is connected to the load via steel wire rope, and the mass of the hook itself cannot be ignored, this causes the hook to undergo primary oscillation at the trolley suspension point, while the load will exhibit secondary oscillation relative to the hook.

With the continuous advancement of automation technology, researchers worldwide have conducted extensive research on the anti-sway control of tower cranes. The main control strategies currently include input shaping, trajectory planning, sliding mode control, fuzzy control, and intelligent control methods [2].

Input shaping technology is a method that divides the control signal into two parts: one part is used to generate a specific control signal to drive the system to move along a predetermined trajectory; the other part is obtained by convolving the control signal from the first part with a specific impulse signal, with the aim of suppressing oscillations caused by underactuation [3]. Trajectory planning is a typical open-loop control technique, the essence of which is to design an ideal trajectory based on the system's control objectives and external constraints [4]. Although open-loop control technology has the advantages of simple structure and easy implementation, it does not consider the system's feedback information during the design process [5]. Moreover, the control effect largely depends on the accuracy of the system model. Therefore, when the system model is inaccurate or subjected to external disturbances, the control effect may be significantly reduced.

Among many closed-loop control methods, sliding mode control technology has good control effects on nonlinear and underactuated systems, and it also has the characteristics of fast response, strong anti-interference ability, and strong robustness [6]. It can effectively deal with uncertainties and external disturbances present in the system. Therefore, this paper chooses the sliding mode control algorithm as the basic control strategy to tackle the complex issues faced by tower cranes, such as underactuation characteristics and state coupling, thereby providing strong assurance for the efficient and stable operation of the crane.

2 THEORETICAL FOUNDATION

2.1 Principle of Sliding Mode Control

Sliding Mode Control (SMC) is a classic nonlinear control strategy that dates back to the 1950s, initially proposed by scholars from the former Soviet Union. The essence of this method is to introduce a specific sliding surface and guide the system's motion through two critical phases: the reaching phase and the sliding phase, using a carefully designed reaching law. During the reaching phase, the system's state moves from any initial position towards the sliding surface; during the sliding phase, the system's state converges to the origin along the sliding surface.

To elucidate the principle of sliding mode control more clearly, consider a nonlinear system as an example. For a controllable n-order system:

$$\begin{cases} \dot{x}_1 = x_2 + v_1(x_1) \\ \dot{x}_2 = x_3 + v_2(x_1, x_2) \\ \vdots \\ \dot{x}_{n-1} = x_n + v_{n-1}(x_1, \dots, x_{n-1}) \\ \dot{x}_n = v_n(x_1, \dots, x_n) + u \end{cases} \quad (1)$$

It is typically possible to decompose it into n first-order subsystems through linear transformation. In the control of

nonlinear systems, backstepping control is a commonly used method that achieves stability by designing a Lyapunov function for the n th subsystem. Specifically, once the n th subsystem is stabilized, its state variable x_n is regarded as a virtual input that affects the $n-1$ th subsystem, and so on, until a reference input u is determined, thereby achieving the stability of the entire system.

In the state space, it is assumed that there exists a hypersurface defined by the function $s(x) = s(x_1, x_2, \dots, x_m) = 0$. Taking a two-dimensional space as an example, this surface divides the state space into three regions: $s(t, x) < 0$, $s(t, x) = 0$, and $s(t, x) > 0$. Here, $s(t, x) = 0$ represents the sliding surface of the system, while $s(t, x) < 0$ and $s(t, x) > 0$ represent the regions on either side of the sliding surface in the state space.

Based on this division, the corresponding sliding mode control law can be designed as follows:

$$u = \begin{cases} u^+(t, x), & s(t, x) > 0, \dot{s}(t, x) < 0 \\ u^-(t, x), & s(t, x) < 0, \dot{s}(t, x) > 0 \end{cases} \quad (2)$$

The core idea is to use the control strategy to guide the system state from the initial position to quickly approach the sliding surface $s(t, x) = 0$, and then slide along this surface until it converges to the desired equilibrium point.

2.2 Reaching Law

When constructing a sliding mode control strategy, it is essential to carefully consider the reachability of the sliding motion and design it in accordance with the principles of improving system performance and reducing chattering. The performance of the sliding mode control system largely depends on the characteristics of the reaching motion because when the system state approaches the switching surface, it has a certain velocity, and this inertia may cause continuous oscillations on the switching surface. By adopting an appropriate reaching law, this chattering problem can be effectively mitigated. The following sections will introduce several common traditional reaching laws:

1. Constant Reaching Law:

$$\dot{s} = -\zeta \operatorname{sgn}(s) \quad (3)$$

2. Exponential Reaching Law:

$$\dot{s} = -\zeta \operatorname{sgn}(s) - ks \quad (4)$$

3. Power Reaching Law:

$$\dot{s} = -\zeta |s|^\alpha \operatorname{sgn}(s) \quad (5)$$

4. General Reaching Law:

$$\dot{s} = -\zeta \operatorname{sgn}(s) - f(s) \quad (6)$$

2.3 Controller Design

This paper employs a simplified dynamic model of the tower crane, which is described in the form of matrix multiplication as follows:

$$M(q)\ddot{q} + C(q, \dot{q})\dot{q} + G(q) = u \quad (7)$$

The system is divided into two parts: fully actuated and underactuated.

$$u_a = M_{a1}(q)\ddot{q}_a + M_{a2}(q)\ddot{q}_u + N_a(q, \dot{q}) \quad (8)$$

$$u_u = M_{u1}(q)\ddot{q}_a + M_{u2}(q)\ddot{q}_u + N_u(q, \dot{q}) \quad (9)$$

Further, it can be obtained that:

$$\ddot{q}_u = -M_{u2}^{-1}(q)[M_{u1}(q)\ddot{q}_a + N_u(q, \dot{q})] \quad (10)$$

$$u_a = (M_{a1} - M_{a2}M_{u2}^{-1}M_{u1})\ddot{q}_a + N_a - M_{a2}M_{u2}^{-1}N_u \quad (11)$$

Firstly, we focus on the anti-sway control issue of the system. By constructing the dynamic model of the hook and the load, we can consider the swing angles of the hook and the load as state variables. Based on these state variables, we can design a sliding mode control strategy to achieve balanced and stable control of the hook and load subsystems. To this end, we incorporate the swing angles of the hook and load, as well as their corresponding swing velocities, into the consideration of the system's internal states, and redefine the system's state variables as $o_1 = q_u, o_2 = \dot{q}_u$, resulting in:

$$\begin{cases} \dot{o}_1 = o_2 \\ \dot{o}_2 = -M_{u2}^{-1}(q)[M_{u1}(q)\dot{q}_a + N_u(q, \dot{q})] \end{cases} \quad (12)$$

Consider the internal dynamic equations for the hook swing angle and the load swing angle separately:

$$\begin{bmatrix} o_2(1) \\ o_2(2) \end{bmatrix} = \begin{bmatrix} \dot{\theta} \\ \dot{\phi} \end{bmatrix} \quad (13)$$

Differentiation yields:

$$\begin{bmatrix} \dot{o}_2(1) \\ \dot{o}_2(2) \end{bmatrix} = -M_{u2}^{-1} \begin{bmatrix} (m_h + m_p)l_1 \cos\theta \ddot{x} + m_p l_1 l_2 \dot{\phi}^2 \sin(\theta - \phi) \\ + (m_h + m_p)g l_1 \sin\theta \\ (m_h + m_p)l_1^2 \ddot{x} - m_p l_1 l_2 \dot{\theta}^2 \sin(\theta - \phi) + m_p l_2 g \sin\phi \end{bmatrix} \quad (14)$$

This leads to further derivation:

$$\begin{bmatrix} \dot{o}_2(1) \\ \dot{o}_2(2) \end{bmatrix} = -\frac{1}{|M_{u2}|} \begin{bmatrix} (m_p l_2^2 (m_h + m_p)) l_1 \cos \theta \ddot{x} + m_p^2 l_1 l_2^3 \dot{\phi}^2 \sin(\theta - \phi) \\ + (m_h + m_p) m_p l_2^2 g l_1 \sin \theta - m_p l_1 l_2 \cos(\theta - \phi) \cdot \\ ((m_h + m_p) l_1^2 \ddot{x} - m_p l_1 l_2 \theta^2 \sin(\theta - \phi) + m_p l_2 g \sin \phi) \\ (m_p l_1 l_2 \cos(\theta - \phi)) (m_h + m_p) l_1 \cos \theta \ddot{x} + m_p l_1 l_2 \dot{\phi}^2 \\ \sin(\theta - \phi) + (m_h + m_p) g l_1 \sin \theta \\ (m_h + m_p) l_1^2 (m_h + m_p) l_1^2 \ddot{x} - m_p l_1 l_2 \theta^2 \cdot \\ (m_h + m_p) l_1^2 (m_h + m_p) l_1^2 \ddot{x} - m_p l_1 l_2 \theta^2 \cdot \\ \sin(\theta - \phi) + m_p l_2 g \sin \phi \end{bmatrix} \quad (15)$$

The selection of the sliding surface is:

$$s = \begin{bmatrix} s_1 \\ s_2 \end{bmatrix} = \begin{bmatrix} k_1 o_1(1) + o_2(1) \\ k_2 o_1(2) + o_2(2) \end{bmatrix} = \begin{bmatrix} k_1 \theta + \dot{\theta} \\ k_2 \phi + \dot{\phi} \end{bmatrix} \quad (16)$$

This further results in:

$$\dot{s} = \begin{bmatrix} \dot{s}_1 \\ \dot{s}_2 \end{bmatrix} = \begin{bmatrix} k_1 o_2(1) + \dot{o}_2(1) \\ k_2 o_2(2) + \dot{o}_2(2) \end{bmatrix} = \begin{bmatrix} k_1 \dot{\theta} - \Delta_{11} \ddot{x} - \Delta_{12} \\ k_2 \dot{\phi} - \Delta_{21} \ddot{x} - \Delta_{22} \end{bmatrix} \quad (17)$$

To enhance the efficiency of sway suppression, this paper employs an exponential reaching law as a method to ensure control performance, ultimately obtaining a closed-loop control linear feedback control law as follows:

$$u^p = k_p^p (x^d - x) - k_d^p \dot{x} + \ddot{x} \quad (18)$$

3 SIMULATION AND ANALYSIS

Figure 1 illustrates a three-dimensional model diagram of the tower crane. In this section, we will first conduct a comparative analysis to verify the superiority of the sliding mode control method proposed in this paper. Furthermore, to assess the robustness and reliability of the model, we will adjust key parameters such as the mass of the trolley and the length of the rope, and observe the system's performance under these changes. Through these tests, we can gain a more comprehensive understanding of the effectiveness and adaptability of the proposed control strategy under various operating conditions.

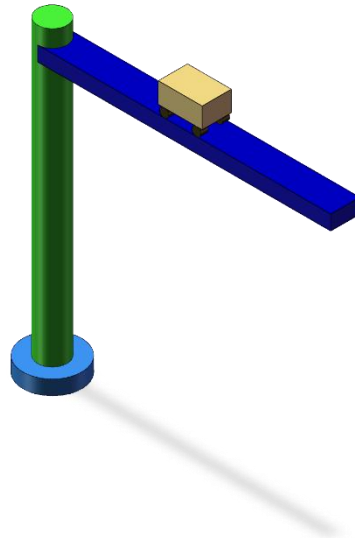


Figure 1 Schematic of the 3D Model of the Tower Crane

3.1 Comparative Analysis

In this subsection, the mass of the trolley, the mass of the load, and the length of the rope are set as follows: $m_t=3\text{kg}$, $m_h=1\text{kg}$, $l=1\text{m}$. The initial conditions are:

$$[q(0) \quad \dot{q}(0)]^T = [0 \quad 0 \quad 0 \quad 0 \quad 0 \quad 0]^T \quad (19)$$

Figure 2 presents a comparison of the effects of applying Sliding Mode Control (SMC) and Proportional Integral Derivative (PID) control in the control system of a tower crane. The figure includes four subplots, representing the changes in position x , the crane arm swing angle α , the cargo radial swing angle θ_1 , and the cargo axial swing angle θ_2 over time. Subplot 2(a) shows the change in position x . It can be observed that both SMC and PID control strategies can bring the position x to the desired value of 1.0 meter, but SMC has a faster response speed, less overshoot, and stabilizes the system state in about 5 seconds, while PID control exhibits more oscillation when approaching the desired value. Subplot 2(b) describes the change in the crane arm swing angle α . The SMC control strategy quickly brings the

crane arm swing angle to the desired value of 0.8 radians and maintains stability, while PID control takes longer to reach a stable state and has significant overshoot in the initial stage. Subplots 2(c) and 2(d) respectively show the changes in the cargo radial swing angle θ_1 and the cargo axial swing angle θ_2 . In these two subplots, the SMC control strategy can more quickly reduce the swing angles to near zero and maintain stability, while PID control shows significant oscillation in the initial stage and takes more time to reach a stable state.

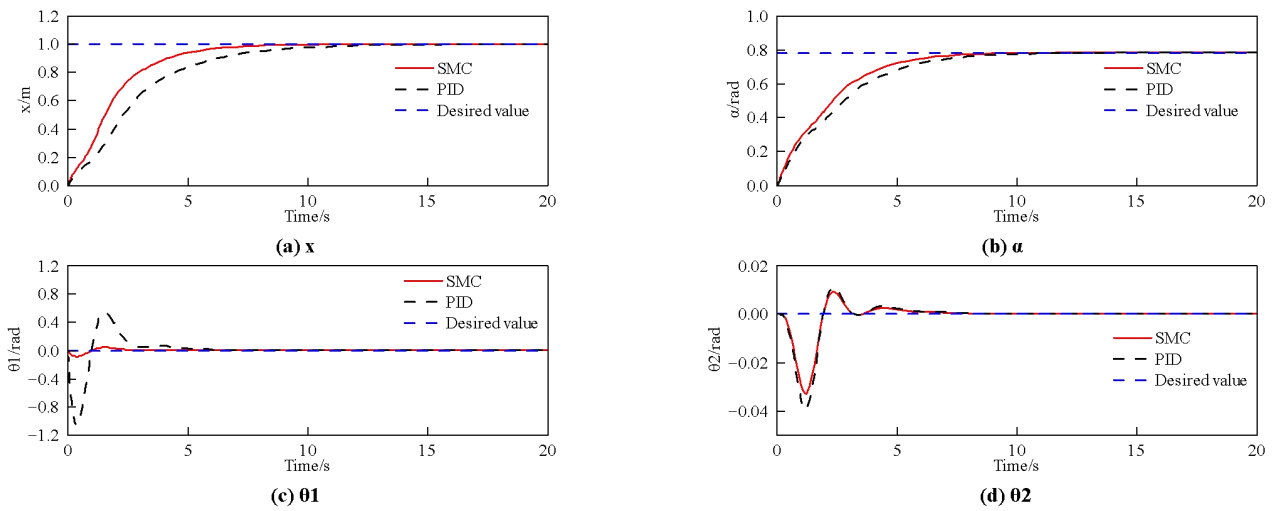


Figure 2 Analysis of Control Results

Overall, SMC is superior to PID control in terms of response speed, overshoot suppression, and stability. Although PID control can ultimately reach the desired state, the oscillation and overshoot during its control process may affect the safety and efficiency of the system. Therefore, SMC provides a better control strategy, especially in scenarios requiring rapid response and high precision.

3.2 Robustness Verification

Figure 3 displays a comparison of the control effects of the sliding mode control model on the trolley system under different parameter settings. Specifically, this subsection sets the trolley mass and rope length to 4kg and 1.5m (Case 1) and 2kg and 0.5m (Case 2), respectively, to verify the effectiveness of the proposed control model. The figure includes four subplots, representing the changes in position x , the crane arm swing angle α , the cargo radial swing angle θ_1 , and the cargo axial swing angle θ_2 over time. Subplot 3(a) shows the change in position x . It can be observed that under both parameter settings, position x can quickly reach the desired value of 1.0 meter, but Case 1 has a slightly faster response speed than Case 2. This indicates that under conditions of greater mass and rope length, the system can reach a stable state more quickly. Subplot 3(b) describes the change in the crane arm swing angle α . Under both parameter settings, the crane arm swing angle α can quickly reach the desired value of 0.8 radians and remain stable. However, Case 2 exhibits greater overshoot in the initial stage, which may be due to the system's insufficient rigidity caused by the smaller mass and rope length. Subplots 3(c) and 3(d) show the changes in the cargo radial swing angle θ_1 and the cargo axial swing angle θ_2 , respectively. In these two subplots, the swing angles under both parameter settings can quickly decrease to near zero and remain stable. However, Case 2 shows greater oscillation in the initial stage, further indicating that smaller mass and rope length may lead to poorer system stability.

Overall, sliding mode control can effectively control the position of the trolley system, the crane arm swing angle, and the radial and axial swing angles of the cargo under different parameter settings, ensuring the system's rapid response and stability. Although the smaller mass and rope length (Case 2) show greater overshoot and oscillation in the initial stage, they still reach a stable state in the end. This indicates that the proposed control model has good adaptability and robustness, maintaining effective control effects under different parameter settings.

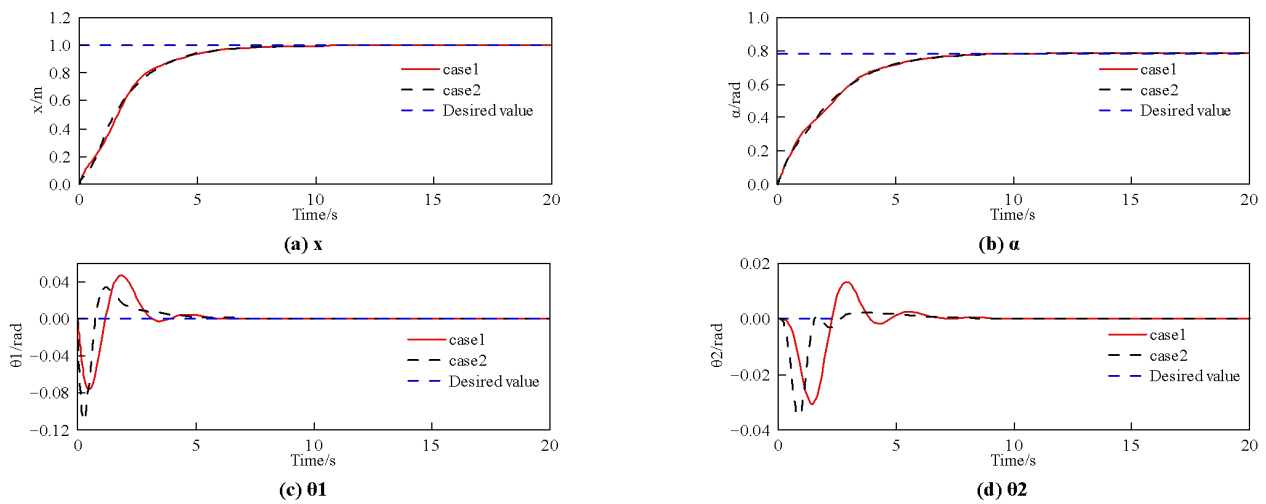


Figure 3 Control Effects Under Different Parameters

4 CONCLUSION

The sliding mode control method proposed in this paper has demonstrated excellent performance in the control of tower cranes. This method can effectively control the displacement of the load, the swing angle of the crane arm, and the radial and axial swing angles of the cargo, ensuring the system's rapid response and stability. Although there are certain oscillations in the initial stage, these oscillations can be quickly suppressed, showing the robustness of the sliding mode controller. This control method is particularly suitable for crane control applications that require high precision and stability. Furthermore, simulation experiments by changing parameters such as the mass of the trolley and the length of the rope have verified the robustness and adaptability of the proposed control model, proving that it can maintain effective control effects under different parameter settings. Therefore, this study provides a new technological approach to the control of tower cranes, which helps to improve the safety and efficiency of their operation.

COMPETING INTERESTS

The authors have no relevant financial or non-financial interests to disclose.

FUNDING

This research was supported by the Shandong Province Technology-based Small and Medium-sized Enterprises Innovation Capability Enhancement Project (Grant No.: 2022TSGC2138).

REFERENCES

- [1] Shao X, Han Y, Zhou L, et al. Linear active disturbance rejection control of double pendulum overhead crane with parameter bandwidth. *Journal of Vibration and Shock*, 2025, 44(04): 82-92.
- [2] Wang S, Sun M, Cao J, et al. Research progress on payload anti-swing control of marine crane. *Journal of Dalian Maritime University*, 2021, 47(04): 1-9.
- [3] Tang Y, Zeng Z, Zhang C. Over-damped ACPD anti-swing control method of double pendulum crane. *Journal of Ordnance Equipment Engineering*, 2024, 45(10): 302-308.
- [4] Lang D, Li Z. Analysis of control methods for tower crane. *Construction Machinery*, 2024, 46(09): 46-50.
- [5] Wang Z, Zhou L, Zheng H. Swing suppression strategy of bridge crane based on fixed-time sliding mode control. *Journal of Mechanical & Electrical Engineering*, 2025, 42(01): 153-163.
- [6] Ge W, Gu J, Cao Y, et al. Anti-swing control of port bridge crane based on fuzzy sliding mode. *Automation & Instrumentation*, 2024, 39(09): 56-60.